Journal of Magnetism and Magnetic Materials 322 (2010) 348–352

Contents lists available at ScienceDirect

Journal of Magnetism and Magnetic Materials

journal homepage: www.elsevier.com/locate/jmmm

Yafet–Kittel-type magnetic ordering in $Ni_{0.35}Zn_{0.65}Fe_2O_4$ ferrite detected by magnetosensitive microwave absorption measurements

G. Alvarez [a,*], H. Montiel [b], J.F. Barron [b], M.P. Gutierrez [c], R. Zamorano [d]

[a] Departamento de Materiales Metálicos y Cerámicos, Instituto de Investigaciones en Materiales, Universidad Nacional Autónoma de México, Apartado Postal 70-360, Coyoacan, DF 04510 México

[b] Departamento de Tecnociencias, Centro de Ciencias Aplicadas y Desarrollo Tecnológico de la Universidad Nacional Autónoma de México, México, DF 04510, México

[c] Universidad Anahuac, México Norte, México DF, México

[d] Departamento de Física, ESFM-IPN, U. P. Adolfo López Mateos Edificio 9, Av. Instituto Politécnico Nacional S/N, Col. San Pedro Zacatenco, 07738 DF, México

ARTICLE INFO

Article history:
Received 22 May 2009
Received in revised form
8 September 2009
Available online 18 September 2009

Pacs:
75.30.Kz
75.50.Gg
76.50.+g

Keywords:
Ni–Zn ferrites
Magnetosensitive microwave absorption
Yafet–Kittel-type canting

ABSTRACT

Magnetosensitive microwave absorption measurements of polycrystalline ferrite $Ni_{0.35}Zn_{0.65}Fe_2O_4$ was carried out at 9.4 GHz (X-band) as a function of temperature. Temperature dependence of the total linewidth (ΔH_{pp}) deduced from the resonance spectra showed the passage through the Curie point ($T_c \sim 430$ K). Additionally, the plot ΔH_{pp} vs. T also indicated the existence of another magnetic phase transition at ~ 240 K, which can be associated with a Yafet–Kittel-type canting of the magnetic moments. Low-field microwave absorption (LFMA) and the magnetically modulated microwave absorption spectroscopy (MAMMAS) were used to give a further knowledge on this material. For low temperature, these techniques give evidence of a Yafet–Kittel-type canting of the magnetic moments.

1. Introduction

The nickel–zinc ferrite system, with nominal formula $Ni_{1-x}Zn_xFe_2O_4$ ($0 \le x \le 1$), is an important family of solid solutions with a remarkable variety of magnetic properties and applications [1,2]. Since zinc tends to occupy tetrahedral (A) sites (Fig. 1), they are "normal" spinels with respect to Zn^{2+}, but the nickel has some preference for octahedral (B) sites (Fig. 1), so they are "inverse" spinels with respect to Ni^{2+}. For $x=0$, i.e. nickel ferrite, A sites are totally occupied by Fe^{3+}, while B sites are shared between Ni^{2+} and the remaining Fe^{3+}. As x increases, Zn^{2+} enters A sites, Ni^{2+} decreases, and Fe^{3+} is distributed among the two sites. This cation distribution leads to large variations in the main superexchange interactions, i.e. A–O–B between A and B sites, and B–O–B between neighboring B sites. For a small content of Zn (x small), A–O–B interactions dominate and the system is ferrimagnetic with a high Curie temperature ($T_c \sim 858$ K for $x=0$), while for $x > 0.9$, B–O–B interactions dominate and the ferrites become antiferromagnetic ($T_N \sim 9$ K for $x=1$). These variations lead as well to a large variety in all the intrinsic magnetic properties (magnetization, crystal anisotropy, magnetostriction, etc.) [1,2].

In addition, a Yafet–Kittel-type canting [3] of the local moments has been proposed to explain a variety of experimental observations such as neutron diffraction [4], magnetic circular dichroism [5] and magnetoresistance [6] in ferrites. In particular, for $Ni_{1-x}Zn_xFe_2O_4$ ferrites with $0.5 < x < 1$, a non-collinear arrangement of the magnetic moments in the A and B sites is expected at low temperatures [4,6]. Fig. 2 illustrates the Yafet–Kittel-type canting, where the B sublattice could be split into two sublattices B_1 and B_2 having magnetic moments equal in magnitude and each making an angle α_{YK} (Yafet–Kittel angle) with the direction of the net magnetization. The Yafet–Kittel temperature (T_{YK}) is defined as the temperature at which the angle α_{YK} vanishes and a parallel arrangement of the B sites appear (and therefore a collinear arrangement between A and B sublattices); i.e. it is a transition from a Yafet–Kittel-type magnetic ordering to ferrimagnetic ordering. In particular, we have chosen $Ni_{0.35}Zn_{0.65}Fe_2O_4$ ferrite, because a magnetic transition from a collinear structure to a non-collinear arrangement of the magnetic moments is expected when diminishing the temperature (with $T_{YK} \ll T_c$) [4,6].

On the other hand, the ferromagnetic resonance (FMR) and electron paramagnetic resonance (EPR) are powerful techniques to investigate the nature of magnetic phases in materials at different temperatures [7–12]. Both ferromagnetic resonance at $T < T_c$, and electron paramagnetic resonance at $T > T_c$, have been

* Corresponding author. Tel.: +52 55 5622 4641.
E-mail address: memodin@yahoo.com (G. Alvarez).

0304-8853/$ - see front matter © 2009 Elsevier B.V. All rights reserved.
doi:10.1016/j.jmmm.2009.09.056

used to investigate Ni–Zn ferrites [7,13]. Recently, the magneto-sensitive microwave absorption around zero magnetic field (low-field microwave absorption, LFMA) has been observed in Ni–Zn [7] and cobalt [14] ferrites. LFMA signal is absent in the paramagnetic phase and emerges as the temperature is decreased below T_c. A complementary method particularly well adapted to study magnetic transitions is the magnetically modulated microwave absorption spectroscopy (MAMMAS) [9,12,15–17]. MAMMAS technique is based on the temperature variations of the modulated microwave power absorption, and provides valuable information about the nature of magnetic ordering [15–17].

In this paper, a systematic study of thermal variations of magnetosensitive microwave absorption for $Ni_{0.35}Zn_{0.65}Fe_2O_4$ ferrite is presented. Resonance parameters allowed the detection of the ferri-paramagnetic transition at ~430 K, and an additional magnetic transition at ~240 K. LFMA results also allow to detect the ferri-paramagnetic transition. For low temperature, LFMA and MAMMAS techniques give evidence of the Yafet–Kittel-type canting of magnetic moments in the B sites.

2. Experimental details

Polycrystalline samples of $Ni_{0.35}Zn_{0.65}Fe_2O_4$ ferrite were prepared by the coprecipitation method from aqueous solutions of $ZnCl_2$, $Fe(NO_3)_3 \cdot 9H_2O$ and $NiCl_2 \cdot 6H_2O$. An aqueous solution of $NaCO_3$ was used as precipitant agent. The chemical reaction was carried out at 60 °C for an hour; the pH was kept ~9–11. The product was sintered at 1000 °C for 80 h. The X-ray diffraction (XRD) of powder samples was obtained with a Siemens D5000 diffractometer using the 1.5406 Å Cu Kα line; XRD measurements were made at 300 K.

The microwave investigations used a JEOL JES-RES 3X spectrometer operating at X-band (9.4 GHz) with 100 kHz modulation. All microwave measurements were carried out in the 150–480 K temperature range. In resonance spectra, the applied DC magnetic field (H_{dc}) could be varied from 0 to 6000 G. LFMA measurements were performed using a Jeol ES-ZCS2 zero-cross sweep unit that digitally compensates any remanence in the electromagnet, allowing the measurements to be carried out by cycling H_{dc} about their zero value, continuously from −1000 to 1000 G with a standard deviation of less than 0.2 G for the measured field. MAMMAS signal was registered with an H_{dc} of 200 G together with amplitude of the modulation field (H_{mod}) of 4 G and an incident microwave power of 5 mW; a slow temperature sweep (~1 K/min) was used. The complete scheme and details concerning the experimental set-up for the MAMMAS and LFMA measurements can be found elsewhere [16,17].

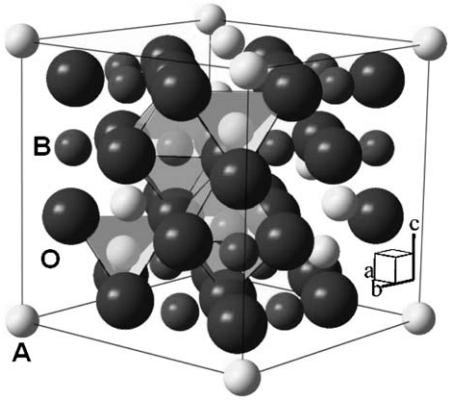

Fig. 1. Schematic representation of unit cell structure for Ni–Zn ferrites; where A and B are tetrahedral and octahedral sites, respectively.

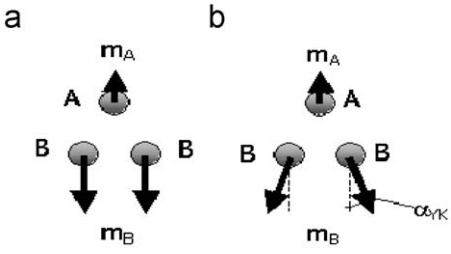

Fig. 2. Spin orientation on the A and B sites, for (a) the collinear and (b) the non-collinear model, in Ni–Zn ferrites; where α_{YK} is the Yafet–Kittel angle.

3. Results and discussion

Fig. 3 shows the XRD pattern of polycrystalline Ni–Zn ferrite. All observed reflection lines were indexed as a single FCC structure corresponding to spinel phase. In Fig. 4, we show the resonance spectra (dP/dH vs. magnetic field) for a few selected temperatures. It can be observed that resonance spectra exhibit a

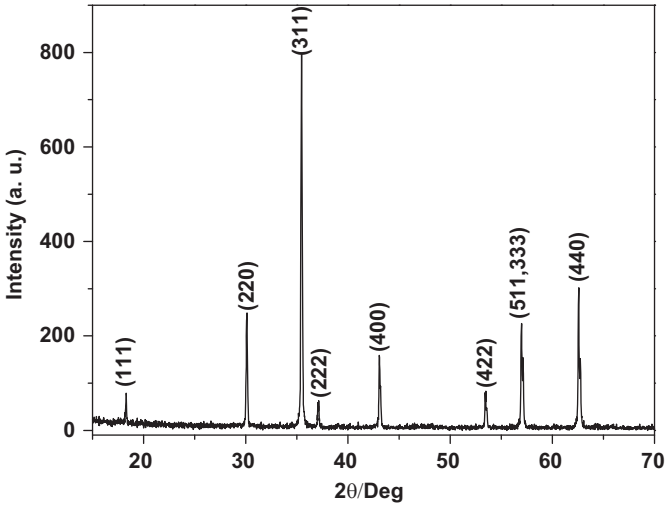

Fig. 3. XRD pattern of polycrystalline sample of $Ni_{0.35}Zn_{0.65}Fe_2O_4$ ferrite.

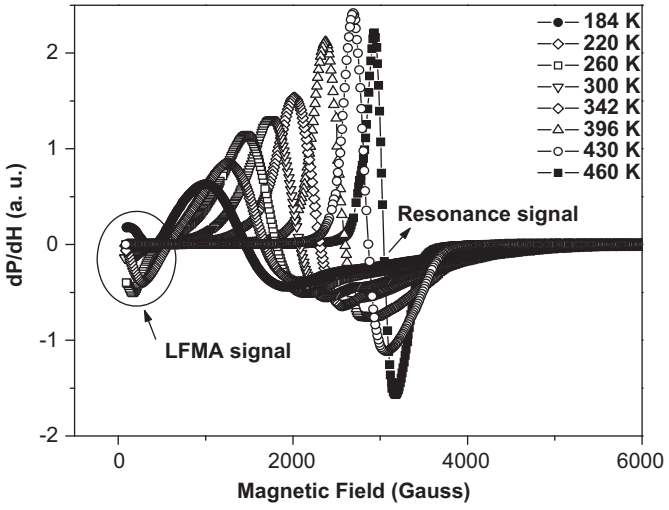

Fig. 4. Resonance spectra of Ni–Zn ferrite for selected temperatures in the 180–460 K temperature range. Note the appearance of LFMA signal (marked by a circle) at $T < 430$ K.

single broad signal in the entire temperature range, a change in their lineshape and a shift in resonant field (H_{res}) are observed when increase the temperature. Starting from low temperature, the asymmetric signal (FMR-mode) gradually changes to a symmetric signal (EPR-mode) with the increase of the temperature, where this change is associated with the Curie transition; i.e. the evolution from ferromagnetic resonance to paramagnetic resonance can be used to determine the Curie temperature (T_c), as we have shown recently in ferrites [7] and it has also been used in the case of the ferrite composites [13].

In a polycrystalline material, the resonance condition for FMR signal is expressed as [18]:

$$\omega = \gamma H_{res} \tag{1}$$

where ω is the angular frequency ($\omega = 2\pi f$), γ is the gyromagnetic ration ($\gamma = eg_{eff}/2m$) and H_{res} is the resonant field, $H_{res} = H_{dc} + H_i$; where H_i is the effective internal field which can be due to many factors (anisotropy—K_1, magnetization—M_S, porosity—p, eddy currents—e, and inhomogenous demagnetization—id), and they are given according to the modified equation by Schlomann [19]:

$$H_i = -\frac{K_1}{2M_S} + 4\pi M_S \frac{p}{1-p} + H_e + H_{id} \tag{2}$$

For a system of randomly oriented crystallites of a magnetic material, we have like a first-order approximation that $H_i = -K_1/2M_S$, i.e. the contribution of the anisotropy field is dominant; with the presence of a large anisotropy field each grain resonates independently, and therefore the resonance curve is a broad envelope of individual grain resonances. In the ferrimagnetic order the internal field is added to the applied field and the resonance condition is reached at low values of H_{dc}, in contrast, in the paramagnetic region, $H_i = 0$ and $H_{res} = H_{dc}$; i.e. when increasing the temperature, see Fig. 5(a), the progressive disappearance of internal field is associate with the lost long-range order.

Srivastava and Patni [20] modified Eq. (2) to indicate all contributions at total linewidth (ΔH_{pp}), and it can be due to many factors particularly in powder samples such as: the magnetization, the sample porosity, the grain size and relaxation times. ΔH_{pp} variations are caused by microscopic magnetic interactions inside the material, mainly the inter particle magnetic dipole interaction and the superexchange interaction. The spin–spin relaxation process is the energy difference transferred to the neighboring electrons and it plays an important role in limiting linewidth; where the behavior of the relaxation time is converse to ΔH_{pp}.

In Fig. 5(b), the decrease in ΔH_{pp} as temperature increases can be explained as due mainly to the weakening of the magnetocrystalline anisotropy as T approaches T_c [21]. The transition appears as an inflection point in plot of $\Delta H_{\rm pp}$ as a function of temperature, as is shown in Fig. 5(b) for our ferrite. The inflection point at $T_c \sim 430$ K is associated with the ferri-paramagnetic transition, this value is in a good agreement with the already reported [22], and that we confirm directly by means of magnetic measurements. Fig. 6 shows the thermal variation of the initial permeability (μ_i) and the saturation magnetization (M_S) through the Curie point. At T_c the long-range magnetic order is completely lost except for some short-range order islands in the material that contribute strongly in the broadening of EPR line. As temperature is increased further into the paramagnetic state, these short-range order islands rapidly decrease in number and size and thus, a narrow and symmetric EPR line is observed at $T > 460$ K.

For the 150–300 K temperature region, Fig. 5(b), a second change in slope at $T_{\rm p} = 240$ K is observed, this inflection point is more apparent in the plot $\mathrm{d}(\Delta H_{\rm pp})/\mathrm{d}T$ vs. T and it is shown as a minimum at $T_{\rm p}$; see the inset of Fig. 5(b). There are two possible explanations for this behavior. The first possibility is that a ferromagnetic impurity in the form of a second phase, with a Curie point close to 240 K and a significant concentration, could explain this behavior; but the DRX spectrum does not show the presence of a second phase. A more sound explanation of this behavior can be attributed to a change in the relative orientation of magnetic moments in A or B sites for this temperature region; i.e. a non-collinear arrangement of the magnetic moments is expected in Ni–Zn ferrite, and that we interpret as a Yafet–Kittel-type canting (Fig. 2); but more evidence is gathered below.

Recently, we have shown that the changes in the FMR/EPR parameters due to magnetic phase transitions can also be detected by MAMMAS measurements [8,9,12,15,17]; where the changes in microwave absorption regime can be associated with

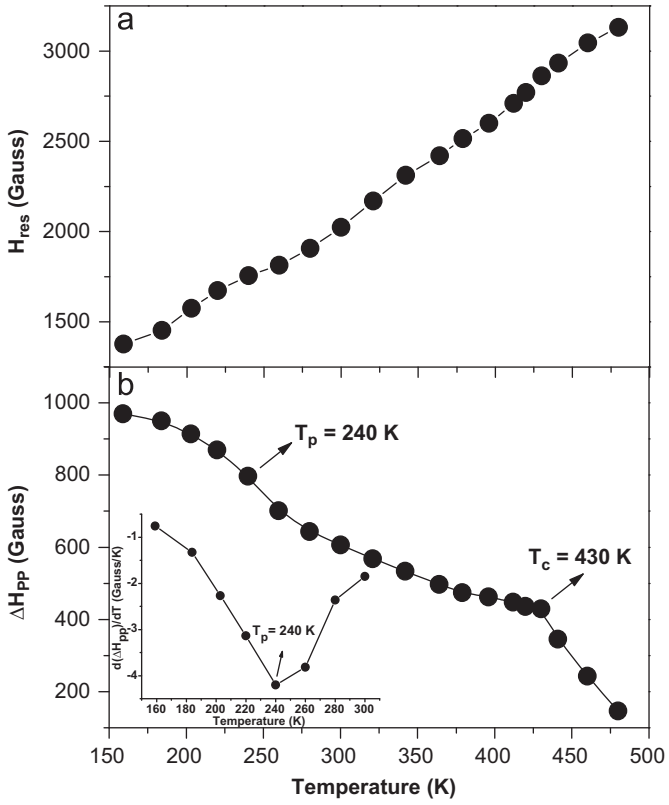

Fig. 5. Temperature dependence of (a) the resonant field (H_{res}) and (b) the total linewidth (ΔH_{pp}) in the 150–480 K temperature range. The inset of Fig. 5(b) shows the temperature dependence of $\mathrm{d}\Delta H_{pp}/\mathrm{d}T$ in the 150–300 K temperature range. The curves connecting points are only guides for the eye.

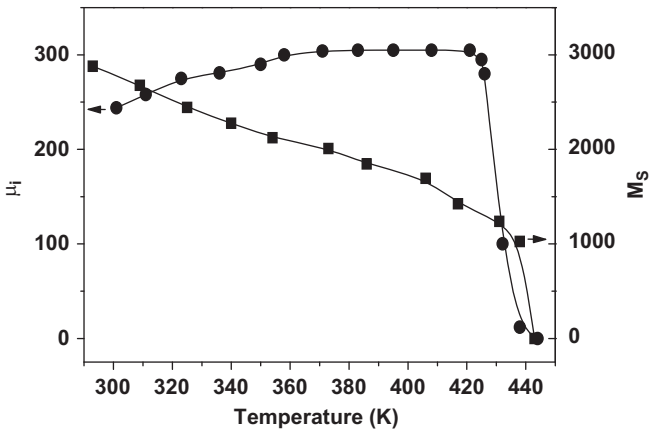

Fig. 6. Curie point measured with the thermal variation of (a) the initial magnetic permeability—μ_i and (b) the saturation magnetization—M_S. The curves connecting points are only guides for the eye.

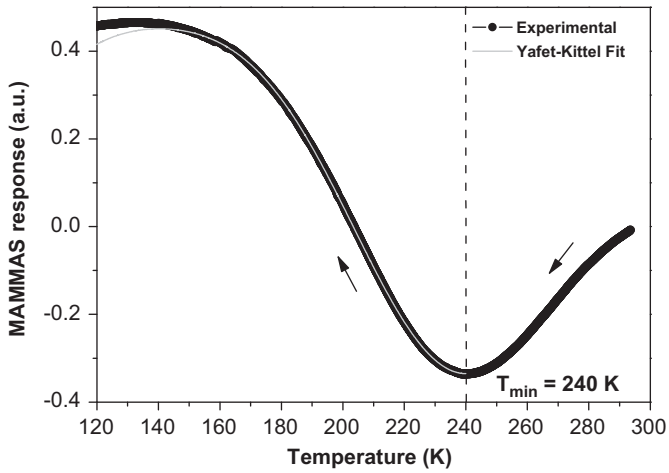

Fig. 7. MAMMAS response of the Ni–Zn ferrite in the 120–300 K temperature range; the solid line correspond to a Yafet–Kittel-type behavior obtained of the fit of Eq. (4).

changes in the absorption dynamics of the magnetic moments, due to a magnetic phase transition [17]. MAMMAS response in the 120–300 K temperature range is shown in Fig. 7, in an attempt to look for a change in microwave absorption due to a magnetic phase transition at low temperature. Starting from room temperature (300 K), as the temperature is decreased, the microwave absorption decreases continuously and it reaches a minimum value at T_{min}=240 K. It is followed by an increasing trend in microwave absorption when temperature continues to decrease. This dynamics indicates that a new magnetic process sets-in, and it starts at $T=T_{min}\approx 240$ K, in a very good agreement with the FMR results. This temperature dependence of MAMMAS response can be understood in terms of a dynamic behavior of magnetic spins. It reveals that for this temperature range, the population of a new kind of absorbing center increases considerably, due to a change of the magnetic coupling; and which it also was suggested from FMR measurements. Additionally, this profile shows that this change appears progressively as temperature is diminished, i.e. it is not a sharp change as could be expected from a structural phase transition. We associate this behavior with a change in the orientation of magnetic moments in A or B sites, which gives rise to a change in microwave absorption dynamics, due to changes in magnetic correlations at $T<T_{\min}$; promoting a Yafet–Kittel-type canting of the magnetic moments in B sites.

For $Ni_{0.35}Zn_{0.65}Fe_2O_4$ ferrite, the part of the interaction energy involving the Yafet-Kittel angle in the molecular-field approximation can be written as [4]

$$E_{YK}=[1.23\alpha+14.44\beta]\cos\alpha_{YK} -[0.12\gamma+17.02\delta+2.89\varepsilon)]\cos 2\alpha_{YK} \quad (3)$$

where α, β, γ, δ and ε are the molecular-field constants that represented the interactions between the A(Fe)–B(Ni), A(Fe)–B(Fe), B(Ni)–B(Ni), B(Fe)–B(Fe), and B(Fe)–B(Ni) sites, respectively. Since the MAMMAS response is related with the microwave power absorption [10,17] and therefore with its energy, we carried a fitting of this response with a similar expression to Eq. (3) for $T\le T_{\min}$, as a first approximation:

$$\text{MAMMAS response} = -0.39\cos[1.81(240-T)] -0.06\cos[2*1.81(240-T)]+0.12 \quad (4)$$

An extremely good fitting is obtained for the 146–240 K temperature range, as is shown in Fig. 7, where we have assumed

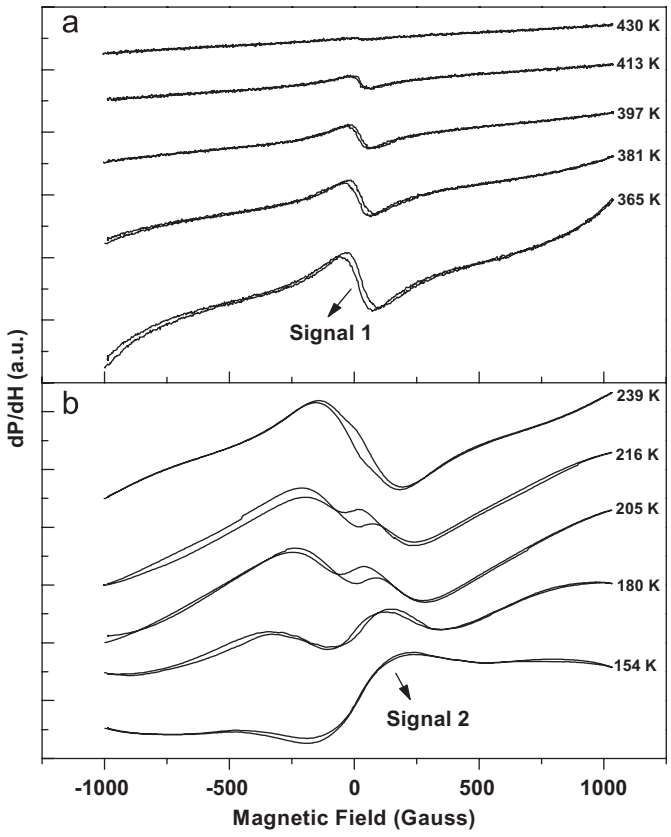

Fig. 8. LFMA spectra for selected temperatures in the (a) 365–430 K and (b) 154–239 K temperature ranges.

that the Yafet–Kittel angle possesses a linear relationship with temperature. In Table 4 of Ref. [4] it appears that, for a composition similar to the one that is studied here, the relationship between the Yafet–Kittel angle and the temperature is effectively linear for a temperature range close to the Yafet–Kittel temperature, and then deviates for low temperatures. MAMMAS profile in Fig. 7, starts to differ from our fit for $T<146$ K, which indicates that the relationship between the Yafet–Kittel angle and the temperature is not linear for these temperatures, in good agreement with Ref. [4].

The whole MAMMAS response depends on the thermal dependence of the spin dynamics, and the intensity of this signal follows the variations on the number of absorption centers (as is suggested by the FMR parameters), in turn is controlled by the establishment of the Yafet–Kittel-type canting of magnetic moments in the B sites at low temperature.

We turn now to LFMA results. Fig. 8 shows LFMA spectra for 154–430 K temperature range. LFMA signal disappears completely at $T>T_c$, see Fig. 8(a), when the long-range order disappears; we can therefore state that LFMA signal is strongly associated with magnetization processes of magnetic phase. For $239\text{ K}<T\le T_c$, LFMA signal exhibits two antisymmetric peaks about zero magnetic field, with the same phase to FMR spectra (which we call signal 1), where a clear hysteresis of this signal appears on cycling the field. For this temperature range, the peak-to-peak value (the difference in magnetic field between maxima and minima peaks—ΔH_{LFMA}) increase slightly when the temperature decreases, as can be seen in Fig. 9; this behavior indicate an increase in the ferromagnetically coupled superexchange interactions in the sample, and that we associate it with the collinear arrangement of B sites.

For $T\le 239$ K, a new LFMA signal (signal 2) is clearly observed in Fig. 8(b). This signal is also centered at zero magnetic field, but

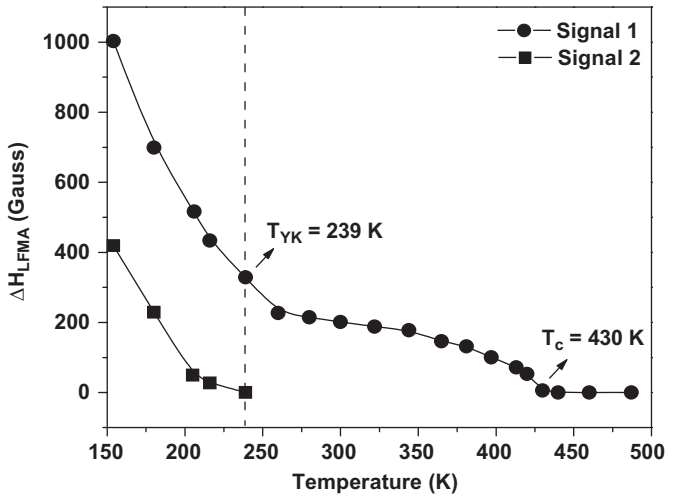

Fig. 9. Behavior of the peak-to-peak width (ΔH_{LFMA}) of LFMA spectra, as a function of temperature in the 150–480 K temperature range.

it exhibits a phase opposite with regard to the signal 1, i.e. with the phase contrary to FMR spectra. This opposite phase (out-of-phase) indicates that the microwave absorption has a minimum value at zero magnetic field, in contrast to the maximum value for signal 1, suggesting a different absorption nature. An out-of-phase signal has been recently observed in ferromagnetic materials [23–25], and we suggest that the signals 1 and 2 are due to absorbing centers with different magnetic ordering. The signal 2 increases with decreasing temperature, starting at $T \leq 239$ K, with a broaden of ΔH_{LFMA} when temperature decreases, as is shown in Fig. 9. For this same temperature region, ΔH_{LFMA} of signal 1 increases continuously with temperature decrease, but now with a higher change rate; this quick broaden might be due to a build-up of short-range magnetic correlations preceding to a magnetic transition. For 154 K, the signal 1 has become practically negligible. The previous dynamics can be attributed to the presence of two different kinds of absorbing centers, and which have a strong magnetic interaction among them. The whole behavior of signals 1 and 2 can be related with a change in the relative orientation of magnetic moments, between the A and B sublattices of the magnetic structure. For the above-mentioned, we propose that the magnetic transition at low temperature is due to the Yafet–Kittel-type magnetic ordering of the moments in the B sites, with an onset temperature T_{YK}=240 K; i.e. for $T < T_{YK}$ the parallel arrangement of the B sites is modified, and a non-collinear arrangement of the magnetic moments in the A and B sites appears, leading to a change in the microwave absorption regime.

4. Conclusions

We have shown that the resonance measurements exhibited the evolution of the resonant absorption from FMR to EPR, when the temperature varies through Curie point (T_c=430 K). Additionally, the FMR parameters indicate the existence of another magnetic phase transition to T_{YK}=240 K, which can be associated with a Yafet–Kittel-type magnetic ordering. MAMMAS and LFMA measurements give evidence of a Yafet–Kittel-type magnetic ordering at low temperature, with a very high detection sensibility.

Acknowledgments

G. Alvarez acknowledges a postdoctoral fellowship from UNAM-Mexico. Support from project of complementary support for SNI-1 of CONACyT-Mexico (No. 89780) and the project PAPIIT-UNAM No. IN116608 are gratefully acknowledged.

References

[1] P. Ravindaranathan, K.C. Patil, J. Mater. Sci. 22 (1987) 3261.
[2] R. Valenzuela, Magnetic Ceramics, Cambridge University Press, Cambridge, 2005.
[3] Y. Yafet, C. Kittel, Phys. Rev. 87 (1952) 290.
[4] N.S. Satya Murthy, M.G. Natera, S.I. Youssef, R.J. Begum, C.M. Srivastava, Phys. Rev. 181 (1969) 969.
[5] W.F. Pong, Y.K. Chang, M.H. Su, P.K. Tseng, H.J. Lin, G.H. Ho, K.L. Tsang, C.T. Chen, Phys. Rev. B 55 (1997) 11409.
[6] A.K.M. Akther Hossain, M. Seki, T. Kawai, H. Tabata, J. Appl. Phys. 96 (2004) 1273.
[7] H. Montiel, G. Alvarez, M.P. Gutiérrez, R. Zamorano, R. Valenzuela, J. Alloys Compd. 369 (2004) 141.
[8] G. Alvarez, R. Font, J. Portelles, R. Valenzuela, R. Zamorano, Physica B 384 (2006) 322.
[9] G. Alvarez, R. Zamorano, J. Heiras, M. Castellanos, R. Valenzuela, J. Magn. Magn. Mater. 316 (2007) e695.
[10] G. Alvarez, H. Montiel, D. de Cos, R. Zamorano, A. García-Arribas, J.M. Barandiarán, R. Valenzuela, J. Non-Cryst. Solids 353 (2007) 902.
[11] G. Alvarez, H. Montiel, D. de Cos, A. García-Arribas, R. Zamorano, J.M. Barandiarán, R. Valenzuela, J. Non-Cryst. Solids 354 (2008) 5195.
[12] G. Alvarez, R. Font, J. Portelles, O. Raymond, R. Zamorano, Solid State Sci. 11 (2009) 881.
[13] K.H. Wu, Y.M. Shin, C.C. Yang, G.P. Wang, D.N. Horng, Mater. Lett. 60 (2006) 2707.
[14] M.E. Mata-Zamora, H. Montiel, G. Alvarez, J.M. Saniger, R. Zamorano, R. Valenzuela, J. Magn. Magn. Mater. 316 (2007) e532.
[15] G. Alvarez, R. Font, J. Portelles, R. Zamorano, R. Valenzuela, J. Phys. Chem. Solids 68 (2007) 1436.
[16] G. Alvarez, R. Zamorano, J. Alloys Compd. 369 (2004) 231.
[17] G. Alvarez, Detection of phase transitions by magnetically modulated microwave absorption spectroscopy, in: Jacob I. Levine (Ed.), Magnetic Materials: Research, Technology and Applications, Nova Science Publishers, New York, USA, 2009.
[18] A.H. Morrish, The Physical Principles of Magnetism, Wiley, New York, 1965.
[19] E. Schlomann, J. Phys. Chem. Solids 6 (1958) 257.
[20] C.M. Srivastava, M.J. Patni, J. Magn. Res. 15 (1974) 359.
[21] T.Y. Byun, S.C. Byeon, K.S. Hong, C. Kyung, J. Appl. Phys. 87 (2000) 6220.
[22] E. Cedillo, J. Ocampo, V. Rivera, R. Valenzuela, J. Phys. E: Sci. Instr. 13 (1980) 383.
[23] Frank J. Owens, J. Phys. Chem. Solids 66 (2005) 793.
[24] H. Montiel, G. Alvarez, I. Betancourt, R. Zamorano, R. Valenzuela, Appl. Phys. Lett. 86 (2005) 072503.
[25] D.K. Aswal, A. Singh, R.M. Kadam, M.K. Bhide, A.G. Page, S. Bhattacharya, S.K. Gupta, J.V. Yakhmi, V.C. Sahni, Mater. Lett. 59 (2005) 728.